



## Low-Temperature Epitaxy of $\text{KTaO}_3$ and $\text{KNbO}_3$ Films

Gregory K. L. Goh,<sup>a,z</sup> Kelvin Y. S. Chan,<sup>a</sup> Barnabas S. K. Tan,<sup>b</sup>  
Y. W. Zhang,<sup>c</sup> J. H. Kim,<sup>d</sup> and Thomas Osipowicz<sup>b</sup>

<sup>a</sup>Institute of Materials Research and Engineering, Singapore 117602

<sup>b</sup>Department of Physics and <sup>c</sup>Department of Materials Science and Engineering, National University of Singapore, Singapore 119260

<sup>d</sup>Department of Materials Science and Engineering, Chonnam National University, Kwangju 500-757, South Korea

Epitaxial perovskite  $\text{KTaO}_3$  films were grown hydrothermally on (100) oriented single-crystal  $\text{SrTiO}_3$  substrates in a 7 M KOH solution at 170°C. Transmission electron microscopy, Rutherford backscattering spectroscopy, and optical measurements showed that despite the low growth temperature, the obtained films were highly crystalline. Also, determination of the residual strain due to grain coalescence, lattice mismatch, and thermal expansion mismatch indicated that differential contraction between the substrate and film during cooling generated sufficient compressive stress to cause film buckling at poorly bonded regions between the film and substrate.

© 2007 The Electrochemical Society. [DOI: 10.1149/1.2801862] All rights reserved.

Manuscript submitted August 22, 2007; revised manuscript received September 28, 2007.  
Available electronically November 8, 2007.

The perovskite  $\text{KTaO}_3$  is an incipient ferroelectric that exhibits a dielectric nonlinearity at low temperatures near the transition temperature of high  $T_c$  superconductors, making it useful as a tunable element in microwave circuits.<sup>1</sup> In addition, due its close lattice match with  $\text{KNbO}_3$ ,  $\text{KTaO}_3$  is ideal as a substrate or buffer layer for the growth of epitaxial  $\text{KNbO}_3$  films.<sup>2</sup> Epitaxial  $\text{KNbO}_3$  films have the largest reported electromechanical coupling constants, making  $\text{KNbO}_3$  highly desirable as surface acoustic wave (SAW) substrates for use as filters in telecommunications and signal processing.<sup>3</sup> Alloying with niobium, the cubic phase of  $\text{KTa}_{1-x}\text{Nb}_x\text{O}_3$  (KTN) is a good candidate material for electro-optic applications, such as band filters, light modulators, and IR detectors, due to its large quadratic electro-optic coefficient and photorefractive effect.<sup>4</sup> Because bulk single crystals of  $\text{KTaO}_3$  and KTN are difficult and expensive to grow, attention has been focused on the growth of epitaxial films.

To date, epitaxial  $\text{KTaO}_3$  films have been grown by pulsed laser deposition while KTN films have also been grown by metallorganic chemical vapor deposition and chemical solution deposition.<sup>2,4,5</sup> These processes require temperatures in excess of 650°C either during deposition or for postdeposition calcination. Alternatively, epitaxial  $\text{KTaO}_3$  films can be grown by a low temperature (<200°C) solution technique known as hydrothermal epitaxy that utilizes aqueous chemical reactions to form heteroepitaxial thin films.<sup>6,7</sup> Generally, high processing temperatures are undesirable because this can lead to interdiffusion and reactions at the film/substrate interface, both of which would be detrimental to device properties. Therefore, the significantly lower processing temperatures employed together with the lower capital and operating costs of the hydrothermal growth method (as vacuum or environmental control equipment are not required) makes understanding the structure and integrity of  $\text{KTaO}_3$  films an important topic.

In a previous report,<sup>6</sup> it was shown that epitaxial  $\text{KTaO}_3$  films can be grown hydrothermally on (100) oriented single-crystal  $\text{SrTiO}_3$  substrates at <200°C. In this study, it is shown by a variety of characterization techniques that despite the low growth temperatures, the as-grown films are of high crystalline quality. In addition, it was observed that buckling cracks were present in the film. In order to understand how this came about, the residual stresses due to grain coalescence, lattice mismatch, and thermal expansion mismatch were examined and corroborated with experimental observations. Identifying the cause of cracking is important for the optimization of the hydrothermal growth parameters needed for the formation of these films.

### Experimental

All reactions were carried out in a 45 mL Teflon-lined, stainless steel hydrothermal reactor (Parr). Films were synthesized on (100) oriented single-crystal  $\text{SrTiO}_3$  substrates (KMT, China) that were polished on one side. The substrate was suspended ~15 mm from the bottom of the Teflon liner with its polished side facing down. To synthesize  $\text{KTaO}_3$ , 0.00025 moles of  $\text{Ta}_2\text{O}_5$  powder (99.99%, Aldrich) and 25 mL of 7 M KOH were introduced into the reactor, which was then placed in a conventional drying oven set at 170°C for 4 h. After the reaction, films were washed with deionized water, isopropanol, and then blown dry in a stream of nitrogen gas.

Film morphology was examined by a scanning electron microscope (JEOL JSM 5600) and atomic force microscopy (Digital Instruments DI3000) while the film thickness was determined by profilometry. The average island size of the film was determined by the linear intercept method (ASTM E1382-97) of a two-dimensional projection of an atomic force micrograph (AFM) of the film surface while the optical properties of the film were determined by variable angle spectroscopic ellipsometry (H-VASE, J. A. Woollam).

Phase identification of precipitated powders was determined by X-ray diffraction (GADDS, Bruker D8) employing  $\text{Cu K}\alpha$  radiation. For the films, X-ray diffraction (XRD) experiments were carried out with a Philips X'pert employing  $\text{Cu K}\alpha_1$  radiation. Lattice parameters of the films were determined from the (002) peak, using the substrate (002) peak as an internal standard. Cross-sectional film samples prepared by conventional wedge techniques were also examined by transmission electron microscopy (TEM) carried out at 200 kV (JEOL JEM 2000EX). Finally, the effect of the  $\text{KTaO}_3$  film on epitaxy in a multilayered  $\text{KNbO}_3/\text{KTaO}_3$  film was also examined by Rutherford backscattering spectroscopy (RBS) using a 2 MeV alpha beam. The RBS depth profiles were fitted with the Rump analysis and simulation package.<sup>8</sup> The details of the hydrothermal  $\text{KNbO}_3/\text{KTaO}_3$  film growth (maximum temperature of 200°C) are found in Ref. 9.

### Results and Discussion

**Microstructure.**—The hydrothermal growth at 170°C of a perovskite  $\text{KTaO}_3$  film with an (100) out-of-plane orientation on the  $\text{SrTiO}_3$  substrate is confirmed by X-ray diffraction (XRD), as shown in Fig. 1a. The film is found to have a lattice parameter of 3.985 Å, quite close to the bulk lattice parameter of 3.989 Å.<sup>10</sup> The XRD also shows that there are no second phases in the film, unlike an earlier work in which films grown at 175°C contained perovskite and pyrochlore phases, both epitaxially related to the substrate.<sup>6</sup> XRD of a  $\text{KTaO}_3$  film grown in this study using the same conditions as in Ref. 6 (i.e., 175°C with 0.0025 moles of  $\text{Ta}_2\text{O}_5$ ) also resulted in a pure

<sup>z</sup> E-mail: g-goh@imre.a-star.edu.sg

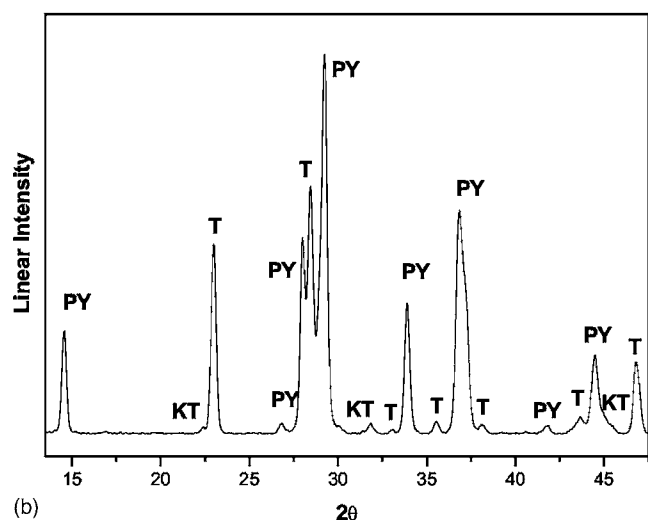
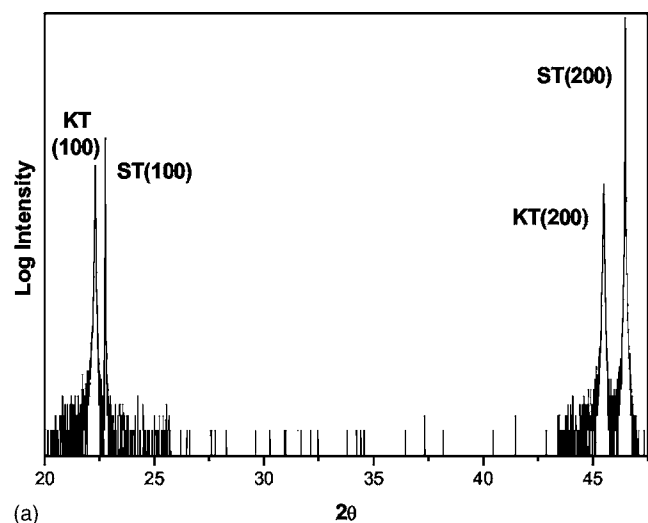


**Figure 1.** XRD pattern of (a)  $\text{KTaO}_3$  film grown at  $170^\circ\text{C}$  after 4 h and (b) powder precipitated simultaneously in solution (T is  $\text{Ta}_2\text{O}_5$ ; ST is  $\text{SrTiO}_3$ ; KT is  $\text{KTaO}_3$ ; PY is pyrochlore).

perovskite film, although the pyrochlore phase was still observed in the precipitated powder for both temperatures employed, as shown in Fig. 1b. This suggests that the different substrate preparations (according to their respective manufacturers, KMT in this study and MTI in Ref. 6) may be responsible for the phase purity of the  $\text{KTaO}_3$  film but this is not investigated further in this study.

Pole figure analysis using the  $\{110\}$  planes of the film (see Fig. 2) and substrate revealed that the  $\text{KTaO}_3$  film grown in this study at  $170^\circ\text{C}$  is epitaxially related to the (100) oriented single-crystal  $\text{SrTiO}_3$  substrate according to  $(100)[001]\text{KTaO}_3// (100)[001]\text{SrTiO}_3$ .  $\omega$ -rocking curve analysis shows that the  $\text{KTaO}_3$  film had a full width at half maximum (fwhm) of  $0.22^\circ$  compared to a value of  $0.04^\circ$  for the substrate, indicating some degree of mosaicity in the film. TEM observations of the film cross section confirms the epitaxial nature of the film and also shows the presence of low angle grain boundaries (arrowed), as shown in Fig. 3. Careful examination of the selected area diffraction (SAD) pattern in Fig. 3b reveals that the diffraction spots are split, indicating the relaxation of residual strain due to lattice mismatch, as will be discussed next.

If an epitaxial film grows coherently on the substrate (i.e., where the periodicity of the film lattice exactly reproduces the periodicity of the substrate), the difference in film and substrate lattice param-

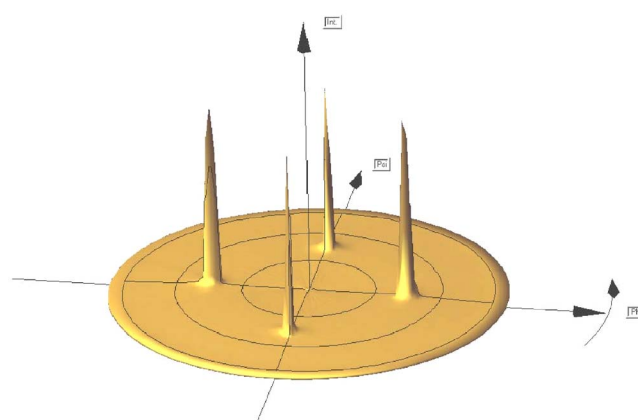


**Figure 2.** (Color online) Pole figure of  $\text{KTaO}_3$  (110) plane revealing the four fold symmetry of the epitaxial film.

eters (lattice mismatch) gives rise to a residual strain. Unless this mismatch is very small or the film is extremely thin, a network of dislocations (misfit dislocations) normally form at or very near the

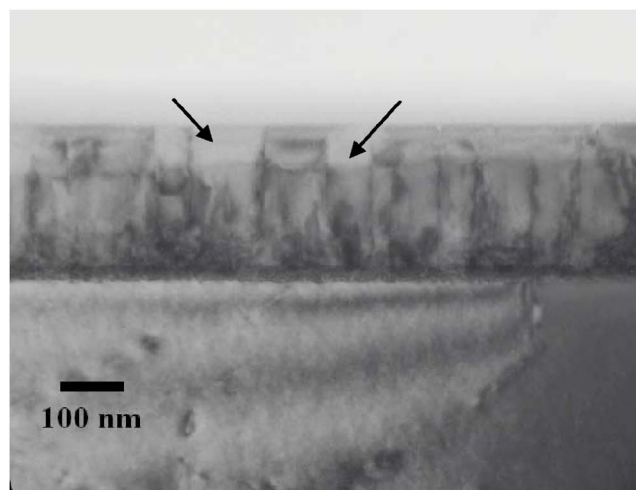


**Figure 3.** (a) TEM of cross section of film/substrate interface (arrows indicate two examples of low angle grain boundaries) and (b) corresponding SAD pattern.

interface to relax most of the mismatch strain. For a given lattice mismatch, misfit dislocations will form above the critical thickness,  $d_c$ , as calculated according to<sup>11</sup>

$$d_c = \frac{Kba_f}{4\pi M\varepsilon_s a_s} \ln\left(\frac{\beta d_c}{b}\right) \quad [1]$$

where the dimensionless constant  $\beta \approx 4$ ,<sup>11</sup> dislocation strength  $b \approx 0.3905$  nm,<sup>11</sup> film lattice parameter  $a_f = 0.3989$  nm, substrate lattice parameter  $a_s = 0.3905$  nm, and lattice misfit strain  $\varepsilon_s = 2.15\%$  for  $\text{KTaO}_3$  on  $\text{SrTiO}_3$ . The biaxial modulus,  $M = E/(1 - \nu) = 490$  GPa (because the film is epitaxial, Young's modulus,  $E$ , and Poisson's ratio,  $\nu$ , are determined from the compliance values,  $s_{ij}$ , for  $\text{KTaO}_3$  as  $E = 1/s_{11} = 395$  GPa and  $\nu = -s_{12}/s_{11} = 0.194$ )<sup>12</sup> while the energy factor,  $K$ , is calculated from the stiffness components,  $c_{ij}$ , according to

$$K = (c_{11} + c_{12}) \sqrt{\frac{c_{44}(c_{11} - c_{12})}{c_{11}(c_{11} + c_{12} + 2c_{44})}} \quad [2]$$

where  $c_{11} = 435$  GPa,  $c_{12} = 104$  GPa, and  $c_{44} = 119$  GPa.<sup>12</sup> The critical thickness according to Eq. 1 was found to be 1.52 nm (approximately four unit cells). Such a small critical thickness indicates that the formation of misfit dislocations is energetically favorable right from the beginning of film growth, and that practically all mismatch strain would have been relaxed for a film that is 261 nm thick, as determined by surface profilometry (this thickness agrees very well with the cross-sectional TEM observation in Fig. 3a that shows a film thickness of  $\sim 260$  nm). Therefore, the splitting of the diffraction spots in the SAD pattern in Fig. 3b should not be unexpected.

In an earlier work,<sup>9</sup> it was shown that the use of  $\text{KTaO}_3$  as a buffer layer improved the epitaxial alignment of the subsequently deposited  $\text{KNbO}_3$  film. Here, Rutherford backscattering spectroscopy clearly demonstrates that epitaxy is maintained in this multilayer  $\text{KNbO}_3/\text{KTaO}_3$  film and also reveals a channeling yield,  $\chi_{\text{min}}$ , of 5%, as demonstrated in Fig. 4b, which compares spectra with random and (100) axially channeled incidence. This compares quite favorably with values of 4–7% observed for films grown by high-temperature (650–750°C) physical vapor deposition methods.<sup>2,13</sup>

To get an idea of the optical properties of the epitaxial  $\text{KTaO}_3$  film, the refractive index,  $n$ , and extinction coefficient,  $k$ , of the film were determined by variable angle spectroscopic ellipsometry (VASE). As shown in Fig. 5a, the refractive index in the 400–800 nm wavelength ( $\lambda$ ) range varied from 2.2 to 2.0 as compared to 2.4 to 2.2 for bulk single crystals.<sup>14</sup> Additionally, the absorption coefficient,  $\alpha$ , was calculated according to,  $\alpha = 4\pi k/\lambda$ . Because the  $\text{KTaO}_3$  system has an indirect bandgap,<sup>15</sup> the optical bandgap,  $E_g$ , was determined by extrapolating the linear portion of the curve obtained by plotting  $(\alpha h\nu)^{0.5}$  vs photon energy ( $h\nu$ ). As shown in Fig. 5b, the present film has an indirect bandgap of 3.87 eV, which compares well to the bulk value of 3.9 eV.<sup>16</sup>

**Film cracking.**—The films were found to contain cracks due to buckling, as shown in Fig. 6. Although films grown by solution routes may crack due to high capillary stresses generated during drying,<sup>17</sup> observation of the film during drying (when the film was still submerged in the wash solvent and after it was dried) by optical microscopy did not reveal any crack formation during drying. Instead, it was observed that the cracks were already present when the film was still submerged in the wash solvent. Furthermore, cracking due to capillary stress is the result of biaxial tension that would lead to a “mud-crack”-type pattern and not the buckling cracks observed here. This indicated that the film either cracked during growth or after cooling, but before the film was dried.

Strain during film growth may arise due to lattice mismatch, accumulation of point defects, and/or grain coalescence. As discussed in the previous section, any strain due to lattice mismatch has been completely relaxed (as demonstrated by the splitting of the

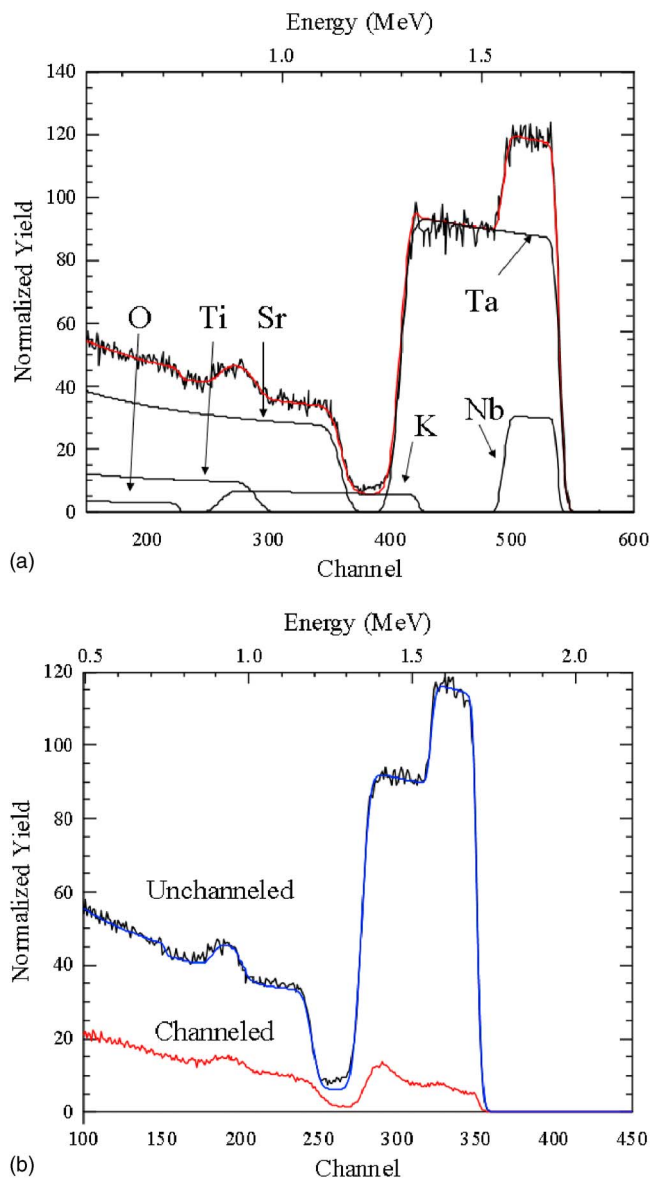


**Figure 4.** (Color online) RBS spectra of multilayer  $\text{KNbO}_3/\text{KTaO}_3$  film showing (a) RUMP simulation of depth profile for unchanneled configuration and (b) comparison of unchanneled and channeled configurations.

spots in the SAD pattern in Fig. 3b) by the formation of misfit dislocations. For established film deposition techniques, methods that generate energetic ions (e.g., rf magnetron sputtering, pulsed laser deposition) lead to films with residual compression due to shallow ion implantation (point defects).<sup>18</sup> In hydrothermal synthesis of perovskite powders, such as  $\text{KNbO}_3$  and  $\text{KTaO}_3$ , incomplete dehydration of intermediate species leads to the incorporation of protons in the lattice, either as hydroxyl ions or water molecules.<sup>19,20</sup> A hydroxyl ion is formed when a proton bonds to a lattice oxygen while the water molecule locates itself at a vacant potassium site in the lattice (potassium and/or tantalum vacancies are required to preserve the overall charge neutrality of the lattice due to the incorporation of protons).<sup>19</sup> These protonic defects and accompanying cation vacancies can reduce the long-range coulomb attractive forces between the ions, leading to the expansion of the lattice.<sup>19</sup> For a film, constraint of this expansion by the substrate could lead to a compressive stress.

For  $\text{KTaO}_3$ , it was demonstrated that perovskite powders synthesized at 150 and 200°C in 15 M KOH solutions experienced lattice

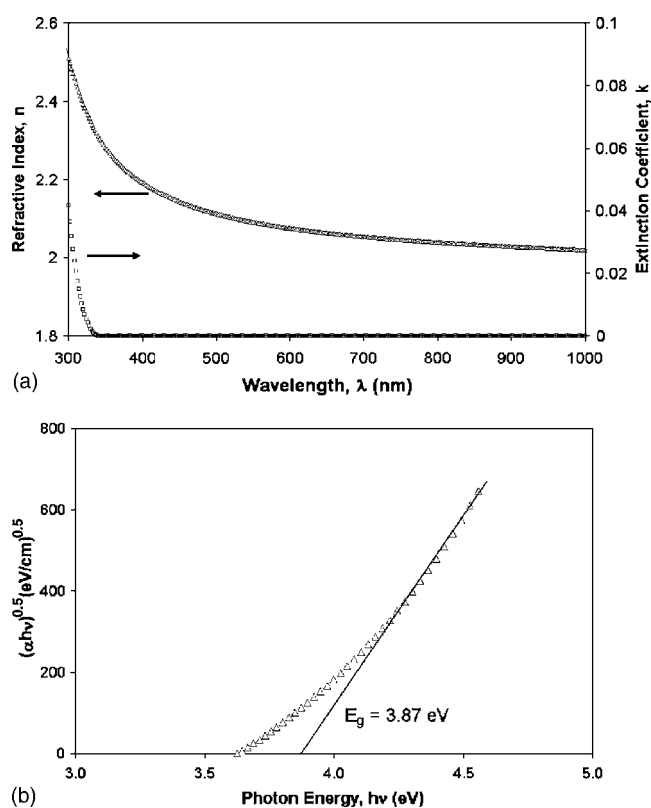


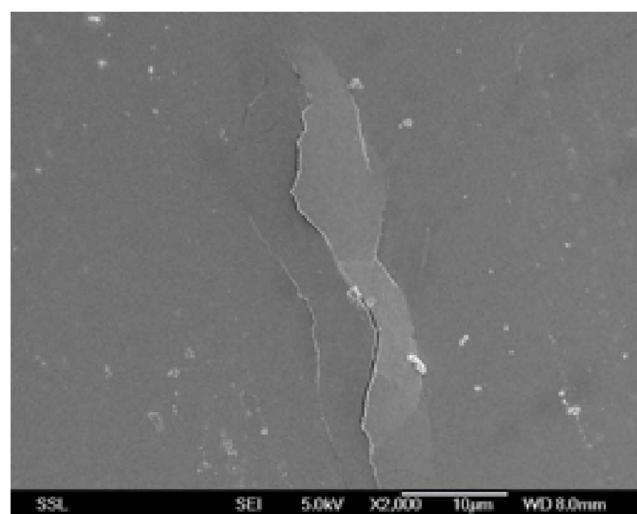
**Figure 5.** Optical properties of the epitaxial  $\text{KTaO}_3$  film: (a) Refractive index and extinction coefficient, and (b) optical bandgap,  $E_g$ .

expansion due to proton incorporation, but that powders synthesized at  $200^\circ\text{C}$  in 7 M KOH solutions did not exhibit an expanded lattice.<sup>19</sup> Although the temperature used in this study was a little lower at  $170^\circ\text{C}$ , the latter study showed that the lattice expansion varied with the KOH concentration and not growth temperature, as the lattice of the powders grown at 150 and  $200^\circ\text{C}$  in 15 M KOH solutions was expanded by the same amount. Also, XRD of the  $\text{KTaO}_3$  film grown in 7 M KOH solutions in this study revealed a lattice parameter of  $3.985 \text{ \AA}$ , comparable to the value of  $3.989 \text{ \AA}$  reported in the literature,<sup>10</sup> confirming the absence of significant lattice expansion in the films. Therefore, it appears that at the end of film growth before cooling, only grain coalescence can contribute to the residual strain or, if the strain energy exceeds the fracture strength, can lead to cracking. Although any strain due to grain coalescence will be tensile in nature, it is still important to estimate this strain as it would offset any compressive strain developed during cooling due to mismatch in the thermal expansion coefficients.

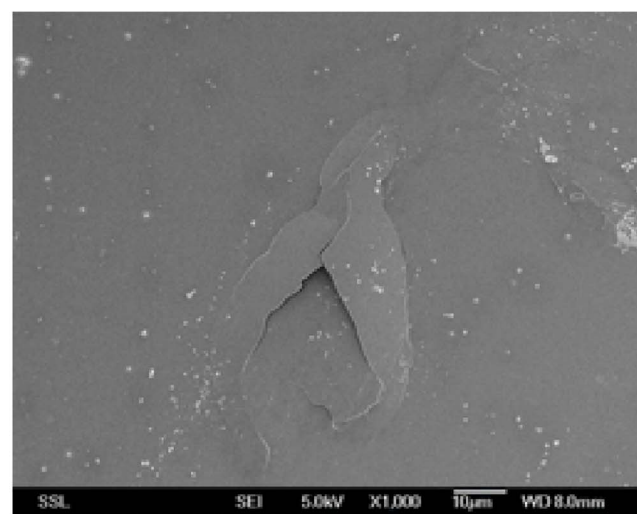
As is commonly observed for growth by low temperature solution methods,<sup>21,22</sup> the film formed by an island growth mode (Volmer–Weber). In the early stages of growth by the Volmer–Weber mode, individual islands nucleate on the substrate, grow, approach, and impinge on adjacent islands, eventually coalescing to form a continuous film. As first proposed by Hoffman,<sup>23</sup> approaching islands with a small gap between them could deform slightly and spontaneously snap together, forming a relatively lower energy grain boundary in place of the two adjacent island free surfaces prior to coalescence. But, the coalescence of islands across the film also results in a tensile strain. For a film with approximately hemispherical grains at the point of coalescence, the average tensile stress can be found using the following<sup>24</sup>

$$\sigma_{\text{ave}} = \frac{4}{R} \left( \gamma_s - \frac{1}{2} \gamma_{\text{gb}} \right) \quad [3]$$

where  $R$  is the average radius of the islands and  $\gamma_s$  and  $\gamma_{\text{gb}}$  are the energies of the island surface and grain boundaries, respectively. For



(a)



(b)

**Figure 6.** SEM micrographs of buckling cracks.

a film under plane stress, the corresponding strain is given by

$$\varepsilon_1 = \frac{4(1-\nu)}{R} \left( \gamma_s - \frac{1}{2} \gamma_{\text{gb}} \right) \quad [4]$$

where the Young's modulus,  $E$ , and Poisson's ratio,  $\nu$ , are 395 GPa and 0.194, respectively, as determined in the previous subsection. Values for the surface and grain boundary energies of  $\text{KTaO}_3$  could not be found in the literature, and as such values for  $\text{SrTiO}_3$ , which is also cubic and paraelectric (such as  $\text{KTaO}_3$ ), were used. From theoretical models,  $\text{SrTiO}_3$  was found to have a surface energy of  $2.44 \text{ J/m}^2$  and a grain boundary energy of  $1.42 \text{ J/m}^2$ .<sup>25,26</sup> From linear intercept analysis of several AFM micrographs (Fig. 7 shows a representative AFM micrograph), an average island radius,  $R$ , of  $0.228 \text{ }\mu\text{m}$  was found. From Eq. 4, the residual tensile strain due to grain coalescence,  $\varepsilon_1$ , is estimated to be about  $6.28 \times 10^{-5}$ .

During cooling from  $170^\circ\text{C}$  to room temperature ( $25^\circ\text{C}$ ), any mismatch in the thermal expansion coefficients (CTE) of the film and substrate can generate a residual strain according to

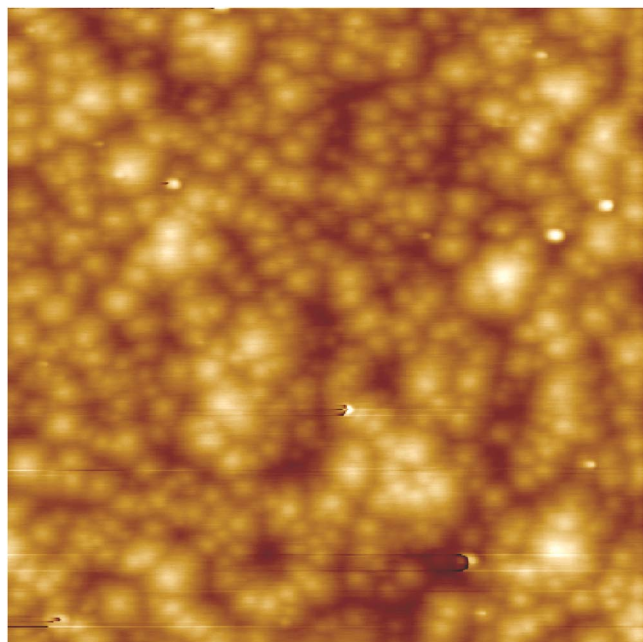


**Figure 7.** (Color online) AFM micrograph of an epitaxial KTaO<sub>3</sub> film grown at 170°C after 4 h (10 × 10 μm image size).

$$\varepsilon_2 = \int_{T_1}^{T_f} (CTE_{\text{film}} - CTE_{\text{substrate}}) dT \quad [5]$$

where  $T_f = 25^\circ\text{C}$ ,  $T_1 = 170^\circ\text{C}$ ,  $CTE_{\text{film}} = 6.8 \times 10^{-6} \text{ K}^{-1}$ , and  $CTE_{\text{substrate}} = 1.1 \times 10^{-5} \text{ K}^{-1}$  are the thermal expansion coefficients of the film and substrate, respectively.<sup>27,28</sup> Because the CTE of the substrate is larger than that for the film and the substrate is much thicker than the film, the resultant compressive strain,  $\varepsilon_2$ , of magnitude  $-6.09 \times 10^{-4}$ , will reside completely in the film. Therefore, at the end of the cooling, the net residual strain,  $\varepsilon_r = \varepsilon_1 + \varepsilon_2 = -5.46 \times 10^{-4}$ , yields a residual stress,  $\sigma_r = M\varepsilon_r = -268 \text{ MPa}$ , i.e., compressive in nature. This is consistent with the observation of buckling cracks that result from the combination of a compressive stress as well as a small separation (e.g., crack or debonding) between the film and substrate.

To further determine if the magnitude of the compressive stress was sufficient to cause the buckling cracks, the cracks shown in Fig. 6 are modeled by a two-dimensional region of width  $2r$  that undergoes buckling if the stress experienced by the film exceeds the critical buckling stress according to<sup>29</sup>

$$\sigma_c = \left[ \frac{\pi^2 E}{12(1 - \nu^2)} \right] \left( \frac{d}{r} \right)^2 \quad [6]$$

where  $d$  is the film thickness. Setting  $\sigma_r = \sigma_c$  and  $d = 261 \text{ nm}$  in Eq. 6, it is found that a value of  $r = 9.26 \text{ μm}$  is sufficient to cause buckling. This value of  $r$  agrees quite well with values in the range of 4–10 μm, observed in Fig. 6, as well as for other observed buckling cracks. Thus, it can be said that the observed buckling cracks are the result of compressive residual stresses developed due to cooling.

Note that a compressive residual stress is a necessary but not sufficient condition to cause buckling. The presence of a separation (crack or debonded region) between the film and substrate is also required. Therefore, if the separation in this study was absent or less

than the critical value determined from Eq. 6 for the given compressive stress level, than buckling would not have occurred. It is believed that the separation at the interface was the result of substrate surface contamination during the predeposition cleaning stage as buckling cracks were no longer observed when substrate cleaning was carried out more thoroughly or if the cleaning and film growth processes were carried out in a clean room environment.

### Conclusion

In this study, pure perovskite KTaO<sub>3</sub> films were hydrothermally epitaxially on (100) oriented single-crystal SrTiO<sub>3</sub> substrates at 170°C, as confirmed by X-ray diffraction and pole figures analysis. X-ray and electron diffraction showed that the highly crystalline film was relaxed while ellipsometry revealed that the film had an indirect bandgap of 3.87 eV. In addition, Rutherford backscattering spectroscopy of a multilayer KNbO<sub>3</sub>/KTaO<sub>3</sub> film showed that the films were highly aligned with a channeling yield of 5%.

The film also contained buckling cracks. It was determined that the compressive strain due to thermal expansion mismatch during cooling after film deposition was significantly larger than the tensile strain due to grain coalescence during film growth such that a net compressive residual stress was present in the film after cooling. This compressive stress together with the presence of separations, due possibly to surface contamination, between the film and substrate at certain locations were responsible for the formation of buckling cracks.

### References

- O. G. Vendik, E. K. Hollmann, A. B. Kozyrev, and A. M. Prudan, *J. Supercond.*, **12**, 325 (1999).
- H.-M. Christen, L. A. Boatner, J. D. Budai, M. F. Chisholm, L. A. Gea, P. Marrero, and D. P. Norton, *Appl. Phys. Lett.*, **68**, 1488 (1996).
- H. Odagawa, K. Kotani, Y. Cho, and K. Yamanouchi, *Jpn. J. Appl. Phys.*, **38**, 3275 (1999).
- B. M. Nichols, B. H. Hoerman, J.-H. Hwang, T. O. Mason, and B. W. Wessels, *J. Mater. Res.*, **18**, 106 (2003).
- K. Suzuki, W. Sakamoto, T. Yogo, and S. Hirano, *J. Am. Chem. Soc.*, **82**, 1463 (1999).
- G. K. L. Goh, C. G. Levi, and F. F. Lange, *J. Mater. Res.*, **17**, 2852 (2002).
- C. K. Tan, G. K. L. Goh, and W. L. Cheah, *Thin Solid Films*, **515**, 6577 (2007).
- L. R. Doolittle, *Nucl. Instrum. Methods Phys. Res. B*, **B9**, 334 (1985).
- G. K. L. Goh and S. K. Donthu, *Mater. Res. Soc. Symp. Proc.*, **718**, D10.13 (2002).
- Powder Diffraction File, Joint Committee on Powder Diffraction Standards, Swarthmore, PA, card no. 38-1470.
- P. A. Langjahr, F. F. Lange, T. Wagner, and M. Rühle, *Acta Mater.*, **46**, 773 (1998).
- A. G. Every and A. K. McCurdy, in *Crystal and Solid State Physics*, D. F. Nelson, Editor, Landolt-Börnstein, Group III, *Low Frequency Properties of Dielectric Crystals*, p. 29[a], Springer, Berlin (1992).
- A. F. Chow, D. J. Lichtenwalner, R. R. Woolcott, Jr., T. M. Graettinger, O. Auciello, A. I. Kingon, L. A. Boatner, and N. R. Parikh, *Appl. Phys. Lett.*, **65**, 1073 (1994).
- S. H. Wemple, *Phys. Rev.*, **137**, 157 (1965).
- T. Neumann, G. Borstel, C. Scharfschwerdt, and M. Neumann, *Phys. Rev. B*, **46**, 10623 (1992).
- M. DiDomenico, Jr., and S. H. Wemple, *Phys. Rev.*, **166**, 565 (1968).
- G. K. L. Goh, S. K. Donthu, and P. K. Pallathadka, *Chem. Mater.*, **16**, 2857 (2004).
- J. S. Speck, A. Seifert, W. Pompe, and R. Ramesh, *J. Appl. Phys.*, **76**, 477 (1994).
- G. K. L. Goh, S. M. Haile, C. G. Levi, and F. F. Lange, *J. Mater. Res.*, **17**, 3168 (2002).
- G. K. L. Goh, F. F. Lange, S. M. Haile, and C. G. Levi, *J. Mater. Res.*, **18**, 338 (2003).
- G. K. L. Goh, X. Q. Han, C. P. K. Liew, and C. S. S. Tay, *J. Electrochem. Soc.*, **152**, C532 (2005).
- G. K. L. Goh, C. G. Levi, J. H. Choi, and F. F. Lange, *J. Cryst. Growth*, **286**, 457 (2006).
- R. W. Hoffman, *Thin Solid Films*, **34**, 185 (1976).
- L. B. Freund and E. Chason, *J. Appl. Phys.*, **89**, 4866 (2001).
- F. Bottin, F. Finocchi, and C. Noguera, *Surf. Sci.*, **574**, 65 (2005).
- S. Hutt, S. Köstlmeier, and C. Elsässer, *J. Phys.: Condens. Matter*, **13**, 3949 (2001).
- G. A. Samara and B. Morosin, *Phys. Rev. B*, **8**, 1256 (1973).
- D. de Ligny and P. Rischet, *Phys. Rev. B*, **53**, 3013 (1996).
- A. G. Evans and J. W. Hutchinson, *Int. J. Solids Struct.*, **20**, 455 (1984).